HHS Public Access

Author manuscript

Mol Cancer Ther. Author manuscript; available in PMC 2015 March 20.

Published in final edited form as:

Mol Cancer Ther. 2014 January ; 13(1): 221–229. doi:10.1158/1535-7163.MCT-13-0561.

Sorafenib suppresses JNK-dependent apoptosis through inhibition of ZAK kinase

Harina Vin[1,*], **Grace Ching**[1,*], **Sandra S. Ojeda**[1], **Charles H. Adelmann**[1], **Vida Chitsazzadeh**[1,6], **David W. Dwyer**[1], **Haiching Ma**[8], **Karin Ehrenreiter**[9], **Manuela Baccarini**[9], **Rosamaria Ruggieri**[10], **Jonathan L. Curry**[2], **Ana M. Ciurea**[3], **Madeleine Duvic**[3,7], **Naifa L. Busaidy**[4], **Nizar M. Tannir**[5], and **Kenneth Y. Tsai**[1,6,7]

[1]Department of Immunology, University of Texas MD Anderson Cancer Center, Houston TX 77030

[2]Department of Pathology, University of Texas MD Anderson Cancer Center, Houston TX 77030

[3]Department of Dermatology, University of Texas MD Anderson Cancer Center, Houston TX 77030

[4]Department of Endocrine Neoplasia, University of Texas MD Anderson Cancer Center, Houston TX 77030

[5]Department of Genitourinary Medical Oncology, University of Texas MD Anderson Cancer Center, Houston TX 77030

[6]Department of Dermatology, University of Texas MD Anderson Cancer Center, Houston TX 77030

[7]University of Texas Graduate School of Biomedical Sciences at Houston, Houston TX 77030

[8]Reaction Biology Corp., Malvern, PA 19355

[9]Max F. Perutz Laboratories, 1030 Vienna, Austria

[10]Feinstein Institute for Medical Research, Center for Oncology and Cell Biology, Manhasset NY 11030

Abstract

Sorafenib is FDA-approved for the treatment of renal cell carcinoma and hepatocellular carcinoma and has been combined with numerous other targeted therapies and chemotherapies in the treatment of many cancers. Unfortunately, as with other RAF inhibitors, patients treated with sorafenib have a 5–10% rate of developing cutaneous squamous cell carcinoma/keratoacanthomas. Paradoxical activation of ERK in BRAF-wild-type cells has been implicated in RAF-inhibitor-induced cSCC. Here we report that sorafenib suppresses UV-induced apoptosis specifically by inhibiting JNK activation through the off-target inhibition of ZAK kinase. Our results implicate suppression of JNK signaling, independent of the ERK pathway, as an additional mechanism of

Corresponding Author: Kenneth Y. Tsai, kytsai@mdanderson.org.
*These authors contributed equally.

Conflicts of Interest: there are no conflicts to declare

adverse effects of sorafenib. This has broad implications for combination therapies using sorafenib with other modalities that induce apoptosis.

Introduction

Sorafenib is a multikinase inhibitor originally designed to target CRAF, but has been found to effectively inhibit multiple kinases including BRAF, VEGFR2, VEGFR3, PDGFRβ, FLT-3, and c-KIT(1, 2). In multiple clinical trials, sorafenib was well tolerated, but commonly associated with dermatologic toxicities, including cutaneous squamous cell carcinoma (cSCC) and keratoacanthomas (KA)(3–7).

All RAF inhibitors tested in clinical trials, including vemurafenib, dabrafenib, and sorafenib, induce hyperproliferative epidermal lesions including cSCC and KA. Vemurafenib appears to have the highest rate: vemurafenib causes KAs and SCCs in approximately 22% of patients (8–10) while sorafenib causes lesions in about 7% of patients(4, 6). Instead, the cutaneous toxicities associated with these RAF inhibitors have been attributed to paradoxical ERK activation, in which *BRAF*-wild-type cells paradoxically activate MEK and ERK activity through increased CRAF activation(11–15). Consistent with this notion, *RAS* mutations are overrepresented in these lesions (particularly for vemurafenib), and combined MEK inhibitor (MEKi) therapy partially suppresses lesion formation(16–19).

However suppression by MEKi may simply reflect an intrinsic need for MEK signaling in this tumor type and paradoxical ERK activation by sorafenib is short-lived for only a few hours, with modest effects on phospho-ERK levels and proliferation in non-target tissues such as keratinocytes in human skin(5). Furthermore, although sorafenib-induced lesions have *RAS* mutations (5), a powerful enabler of paradoxical ERK activation, they were found in a small minority of samples, significantly less frequently than in vemurafenib-induced lesions(16, 17). Therefore, we sought to identify whether there might be other mechanisms contributing to sorafenib-induced cSCC.

Materials & Methods

Cell Culture and UV Irradiation

HaCaT cells were originally obtained from Norbert Fusenig (German Cancer Research Center) and cultured in DMEM/Ham's F12 50/50 (Cellgro) supplemented with 10% Fetal Bovine Serum (FBS) (Sigma), glutamine, and Primocin (Invivogen). NHEKs (Lonza) were cultured in media according to manufacturer's instructions. Irradiation was performed using an FS40 sunlamp dosed by an IL1700 radiometer. Following irradiation, cells were treated with sorafenib (LC Laboratories) or DMSO (1:2000).

Flow Cytometry

Adherent cells were trypsinized and non-adherant cells collected for staining with Annexin V, TMRE, and Cytox Blue. TMRE (Invitrogen) was used as a measure of mitochondrial membrane potential, Annexin V-APC (Invitrogen) as a probe for apoptosis, and Cytox Blue (Invitrogen) as an indicator for dead cells. Data was collected and analyzed using a flow

cytometer (FACScalibur, Becton Dickinson) and FlowJo Software (Tree Star). Data were calculated and charts were plotted using GraphPad Prism 5 software.

Western Blot Analysis

Cell were lysed in standard buffers with protease inhibitors (Roche) and phosphatase inhibitors (Santa Cruz) with extracts run on SDS/polyacrylamide gels and transferred to Immobilon-P transfer membrane (Millipore). Blots were blocked in TBST (10mM Tris-HCL pH8, 150mM NaCl, 0.5% Tween) containing 2.5% BSA, probed with primary antibodies (all Cell Signaling), corresponding HRP-conjugated secondary antibodies, and signals detected using ECL kit (Amersham).

Lentiviral Knockdown Experiments

Lentiviral shRNA knockdown was accomplished using standard lentiviral methods using 293T cells and psPAX2 and VSVG packaging plasmids. shRNA clones against ZAK (clones: V2LHS_239842; V3LHS_336769) and TAOK2 (clone: V3LHS_315551), as well as a non-silencing shRNA were obtained from Open Biosystems in the GIPZ vector. Following transduction, cells were puromycin-selected to obtain a stably infect population and FACS sorted to obtain cells with high-level suppression. Degree of mRNA suppression was quantified by qPCR using Taqman probes using internally controlled (2-color, same well) GAPDH probes to ensure proper normalization.

Mice experiments

For chronically-irradiated Hairless mice, 3 month-old females were irradiated thrice weekly for a total weekly dose of 12.5 kJ/m^2 UVB (solar simulator, Oriel). At 72 days, sorafenib treatment was started by oral gavage (12.5% Cremphor, 12.5% ethanol in water) at 50 mg/kg per day.

Immunohistochemistry

Cutaneous squamous cell carcinomas biopsied from patients treated with or without sorafenib were obtained under IRB approval (LAB08-0750). Staining levels were quantified by counting positively labeled cells and dividing by the total area of the tumor tissue (malignant keratinocytes) within each sample. To measure tumor areas, all samples were photographed, tumor cells outlined, and total pixel numbers calculated using image analysis tools in Adobe Photoshop and standardized to a hemacytometer to convert to mm^2.

Soft agar assays

For growth assays, transformed and immortal cells were generated by retroviral infection. WT MEFs and *Craf*−/− MEFs infected with HRAS (pBABE puro HRASV12) and E1A (pLS adenovirus E1A-12S) expressing lentiviruses were selected with puromycin. Cells were seeded in soft agar at 2×10^3 in 24-well plate format in growth medium containing 0.3% agar over a base layer of 0.6% agar, with varying concentrations of sorafenib or with dimethylsulfoxide (Sigma-Aldrich) vehicle control.

Results

Sorafenib suppresses UV-induced apoptosis in keratinocytes

Because many of the cSCC/KA induced by RAFi occur on sun-exposed areas, we hypothesized instead that sorafenib could affect UV-induced apoptosis. When we exposed HaCaT keratinocyte cell lines and primary normal human epidermal keratinocytes (NHEK) to 500 J/m^2 of UVB, they underwent significant apoptosis by 24 hours (Fig. 1A–B) as assessed by FACS for Annexin V+; TMRE (tetramethylrhodamine)-low cells. Treatment with 1 μM sorafenib resulted in significant suppression of apoptosis as compared DMSO-treated controls, by 40% for HaCaT cells (51.0±3.6 % vs. 30.6±4.1 %) and 81% for NHEKs (34.5±1.8 % vs. 6.6±0.5 %) (Fig. 1A–B).

The stress-activated c-Jun N-terminal (JNK) MAP kinase pathway is critically important in UV-induced apoptosis(20), so we explored its activation in cells treated with and without sorafenib post UV irradiation. Phospho-JNK levels were highly induced in DMSO-treated cells following UV irradiation, and potently suppressed in the presence of 1 μM sorafenib. Phosphorylation of MKK4 (MAP2K4) and MKK7 (MAP2K7), two kinases required for the activation of JNK(21–23), were also upregulated significantly by UV treatment particularly at 1 and 6 hours (lanes 3, 5, 7; Fig. 1C) and suppressed by drug treatment (lanes 4, 6, 8; Fig. 1C). ERK signaling, as seen by phospho-ERK levels, remained intact, with paradoxical hyperactivation following sorafenib treatment (Fig. 1C).

Sorafenib suppresses apoptosis and JNK signaling independently of ERK activation

Because sorafenib exerts potent effects on ERK signaling(5, 14), we sought to probe whether its suppression of JNK-dependent apoptosis could be the result of cross-talk between ERK and JNK signaling. Because sorafenib induces a dose dependent activation of the MAP kinase pathway in *BRAF*-wild-type cells(5, 14), we separated the effects on ERK signaling by simultaneously treating cells with the MEK inhibitor selumetinib(24). NHEK cells and HaCaT cells were treated with sorafenib singly and in combination with selumetinib and then UV irradiated. Sorafenib suppressed UV-induced apoptosis strongly, regardless of whether selumetinib was present (Fig. 2A–B). Selumetinib did not effect sorafenib-mediated suppression of apoptosis or JNK activation (lanes 5–8; Fig. 2C–D) despite potent abrogation of ERK phosphorylation (lanes 3–4, 7–8; Fig. 2C–D).

Multiple upstream kinases of JNK are inhibited by sorafenib

We then sought to determine how sorafenib suppresses JNK activation and apoptosis. Given that MKK4 and MKK7 activation were also suppressed at 1 μM sorafenib (Fig. 1C,D), we reasoned that sorafenib must affect upstream kinases. Comprehensive kinase profiling of sorafenib has been reported using a quantitative binding assay platform(25, 26); therefore we performed *in-vitro* kinase assays against a panel of 38 kinases reported to be upstream of JNK (21, 27) and other kinases previously tested against sorafenib using a 10-dose, 3-fold serial dilution starting at 10 μM (Supplementary Table 1). None of the JNKs is directly inhibited.

We identified ZAK, TAO1/TAOK2, MAPK14 (p38α) and MAPK11 (p38β) as having low *in-vitro* IC50s below 500 nM (Supplementary Table 1). Using p38 inhibitors BIRB796 and LY2228820, we were unable to observe any suppression of UV-induced apoptosis (data not shown). Therefore, we focused on ZAK and TAOK2, which have the lowest biochemical IC50s of 48.6 nM and 59.8 nM, respectively (Fig 3A–B). These IC50s are in the same nanomolar range as those previously reported for BRAF and CRAF(2) and in our panel of assays (Supplementary Table 1).

ZAK is critically important for JNK activation upstream of MKK4 and MKK7(28) and is important for doxorubicin-induced apoptosis(29, 30). TAOK2 has been implicated to be an activator of JNK as well(31–35). To examine the requirements for ZAK and TAOK2 in promoting JNK activation and apoptosis more directly, we performed lentiviral shRNA knockdown experiments in HaCaT cells. HaCaT cells with >85% knockdown of ZAK kinase by qRT-PCR (Taqman; (Fig. 3C) were created using two lentiviral shRNA clones (pGIPZ, Thermo), ZAK-1 and ZAK-4. Cells expressing shRNA ZAK-1 were then infected to express shRNA against TAOK2 as well (Fig. 3C). Both ZAK single knockdown and ZAK/TAOK2 double knockdown cells lack detectable ZAK protein expression and ZAK/TAOK2 double knockdown cells showed 91% reduction in TAOK2 mRNA (Taqman; Fig. 3C). Cells expressing shRNA ZAK-1 and ZAK-4 were substantially more resistant than scramble shRNA-expressing (SCR) cells to UV-induced apoptosis (Fig. 4D). Knockdown of ZAK alone essentially accounted for the entire effect of sorafenib on UV-induced apoptosis (Fig. 4D). ZAK-1-shRNA-expressing HaCaT cells showed statistically significant, but small differences in suppression of apoptosis as compared to ZAK/TAOK2 double knockdown (12%) and sorafenib-treated SCR cells (17%) (Fig. 3D). Importantly, JNK activation was substantially suppressed in ZAK-1-shRNA and ZAK/TAOK2 double knockdown cells at 1 hr and 6 hr post-irradiation (Fig. 3E). The suppression is most evident by treatment with 1 μM sorafenib (lanes 6, Fig. 3E) but it is clear than both single ZAK knockdown and double ZAK/TAOK2 knockdown both result in significant suppression of phospho-JNK (lanes 7, 8; Fig. 3E).

Sorafenib suppresses JNK activation and apoptosis *in-vivo*

To address whether sorafenib-mediated suppression of JNK signaling and apoptosis occurs *in-vivo*, we examined cSCC arising in patients treated with sorafenib and compared them to sporadic cSCC that were histologically similar, arising in individuals never treated with vemurafenib (Fig. 4A–D). Phospho-JNK and cleaved caspase-3 expression were probed using immunohistochemistry and quantified following normalization by unit area (mm^2) of tumor tissue (malignant keratinocytes) only (Fig. 4A–E). Sporadic cSCC arising in patients never treated with sorafenib (n=9) had substantially greater expression of phospho-JNK (p=0.0045; Fig. 4A, E) and cleaved caspase-3 (p=0.003; Fig. 4B, E) as compared to lesions arising in sorafenib-treated patients (n=13; Fig. 4C, D, E). Therefore, there are significant reductions in phospho-JNK (46%) and cleaved caspase-3 expression (88%) in human cSCC, showing that suppression of JNK activity and apoptosis occur *in-vivo* in patients treated with sorafenib.

To model the emergence of UV-driven cSCC under controlled conditions, we exposed 2 cohorts of Hairless mice to chronic low-dose (12.5 kJ/m^2 weekly) UV using solar simulators (Oriel). In this model of UV-driven cSCC development, we irradiated the mice for 72 days prior to initiation of drug (50 mg/kg daily, oral gavage) or control vehicle treatment. Papillomas were observed within 30 days of drug administration and although the kinetics of lesion development were similar, drug-treated animals had 2.3-fold more lesions ($p<10^{-4}$; Fig. 5A–B). Lesions were well-differentiated papillomas (Fig. 5C), some of which progressed to invasive SCC. When we quantified the effects of sorafenib on JNK activation and apoptosis in these papillomas and cSCC, we found decreases in both phospho-JNK expression (30%, p=0.28, n=6 pairs) and cleaved caspase 3 expression (80%, p=0.03, n=6 pairs; Fig. 4E) in sorafenib-treated mice as compared to control-treated mice.

Paradoxical ERK activation is separable from JNK activity suppression

While the effects of sorafenib on JNK-dependent apoptosis is clear and independent of ERK activity (Fig. 2), the relative contribution of paradoxical ERK activation vs. JNK pathway inhibition to tumorigenesis has not been precisely addressed. To study this, we used the fact that paradoxical ERK activation requires *CRAF*(11–13). We used isogenic, matched wild-type (WT) and *Craf*-deficient (*Craf*−/−) mouse embryonic fibroblasts (MEFs) and transformed them with adenovirus E1A and human $HRAS^{G12V}$ to enable anchorage-independent growth. WT and matched *Craf*-deficient MEFs were plated in soft agar assays(16) and treated with sorafenib. Both WT and *Craf*-deficient MEFs exhibited a significant colony formation advantage in the presence of sorafenib (compare Fig. 6A and 6C; 6B and 6D). When normalized to untreated transformed WT and *Craf*−/− MEFs, sorafenib treatment resulted in a 1.92-fold expansion of colony numbers in WT MEFs and a 1.66-fold expansion in *Craf*−/− MEFs. Based upon this analysis, we estimated that the effect of paradoxical ERK activation to be 13.5% and other effects, including inhibition of JNK activity, to account for the rest (86.5%) of the total colony growth advantage (Fig. 6E).

Discussion

The selectivity of kinase inhibitors remains a crude estimate of the entire spectrum of potential biological effects. Although sorafenib is not generally regarded as being highly selective, its inhibition of several kinases relevant for cancer cell signaling likely contributes to its clinical efficacy *in-vivo*(1), and it is still unclear to what extent individual targeted kinases contribute to the observed efficacy in certain settings(36). What has remained relatively underexplored in the study of targeted inhibitors is how unintended targets such as ZAK kinase affect the biology of non-target cells (keratinocytes).

The prevailing explanation for why cSCCs are accelerated in RAF-inhibitor-treated patients is paradoxical ERK activation, which occur most prominently in cells with mutant *RAS*. *RAS* mutations occur, along with mutations in *TGFβR1* and *TP53*, in cSCC arising in sorafenib-treated patients(4, 5); however *RAS* mutations do not appear to be as over-represented as they are in vemurafenib-induced lesions(16, 17), perhaps suggesting that the relative contribution of paradoxical ERK activation may be lower in sorafenib-exposed cells. Furthermore, paradoxical ERK activation appears to be short-lived(5). Therefore, these

findings also suggest that other mechanisms play a role in accelerating the development of cSCC.

We have discovered a novel effect of sorafenib in inhibiting UV-induced JNK activation and apoptosis. This effect is independent of ERK signaling, and is not the result of paradoxical ERK activation observed with RAF inhibitors. After profiling several kinases upstream of JNK and p38, we showed that TAOK2 and ZAK kinases were the most likely targets and that inhibition of ZAK kinase is predominantly responsible for this effect. Sorafenib has been previously shown to suppress ZAK kinase and downstream JNK signaling(28–30). Indeed, multiple inhibitors are known to inhibit ZAK kinase including nilotinib(30), suggesting it may be a promiscuous target of multiple small molecule kinase inhibitors. Whether this is due to structural similarities is not currently known.

We show for the first time that sorafenib suppresses JNK-dependent UV-induced apoptosis in cells, in squamous lesions in both treated patients and mice, and contributes to a significant portion of the acceleration of soft agar colony formation *in-vitro*. cSCC arising in patients treated with sorafenib have substantially less phospho-JNK expression and apoptosis than sporadic cSCC arising in patients never treated with sorafenib (Fig. 4). Similarly, in our mouse model of UV-driven cSCC, both phospho-JNK expression and cleaved caspase-3 expression are inhibited by sorafenib (Fig. 5). Finally, we employed a soft agar colony assay to test the relative contributions of paradoxical ERK activation and JNK-mediated apoptosis by using *Craf*-deficient MEFs which do not exhibit paradoxical ERK activation. In this assay, paradoxical ERK activation played a small role in colony growth (Fig. 6). However, our findings do not exclude an absolute requirement for either paradoxical ERK activation or JNK inhibition in the acceleration of cSCC development; our results show that both cooperate in this process. Our results have important implications for the effects of sorafenib on non-target tissues and suggests that toxicities that are related to JNK signaling may be impacted significantly by sorafenib.

Supplementary Material

Refer to Web version on PubMed Central for supplementary material.

Acknowledgments

The authors acknowledge the assistance of Trellis Thompson in initial cell culture experiments, Sherie Mudd, Humaira Khan, Hafsa Ahmed, and Patricia Sheffield for histology, Nasser Kazimi and Omid Tavana for assistance in UV radiation experiments, and the South Campus Vivarium for mouse maintenance. K.Y.T. acknowledges Ronald P. Rapini for departmental support as well as Tyler Jacks, Gordon B. Mills, Patrick Hwu, and Jeffrey N. Myers for critical discussions and mentorship. K.Y.T. acknowledges the funding support of DX Biosciences Cancer Research Fund, MD Anderson Cancer Center IRG Program, American Skin Association, Elsa U. Pardee Foundation, institutional funds, and NCI CA16672 (FACS, Characterized Cell Line, and Genomics Cores).

References

1. Iyer R, Fetterly G, Lugade A, Thanavala Y. Sorafenib: a clinical and pharmacologic review. Expert Opin Pharmacother. 2010; 11:1943–55. [PubMed: 20586710]
2. Wilhelm SM, Carter C, Tang L, Wilkie D, McNabola A, Rong H, et al. BAY 43-9006 exhibits broad spectrum oral antitumor activity and targets the RAF/MEK/ERK pathway and receptor

tyrosine kinases involved in tumor progression and angiogenesis. Cancer Res. 2004; 64:7099–109. [PubMed: 15466206]

3. Autier J, Escudier B, Wechsler J, Spatz A, Robert C. Prospective study of the cutaneous adverse effects of sorafenib, a novel multikinase inhibitor. Arch Dermatol. 2008; 144:886–92. [PubMed: 18645140]
4. Arnault JP, Wechsler J, Escudier B, Spatz A, Tomasic G, Sibaud V, et al. Keratoacanthomas and squamous cell carcinomas in patients receiving sorafenib. J Clin Oncol. 2009; 27:e59–61. [PubMed: 19597016]
5. Arnault JP, Mateus C, Escudier B, Tomasic G, Wechsler J, Hollville E, et al. Skin tumors induced by sorafenib; paradoxic RAS-RAF pathway activation and oncogenic mutations of HRAS, TP53, and TGFBR1. Clin Cancer Res. 2012; 18:263–72. [PubMed: 22096025]
6. Dubauskas Z, Kunishige J, Prieto VG, Jonasch E, Hwu P, Tannir NM. Cutaneous squamous cell carcinoma and inflammation of actinic keratoses associated with sorafenib. Clinical genitourinary cancer. 2009; 7:20–3. [PubMed: 19213663]
7. Kong HH, Cowen EW, Azad NS, Dahut W, Gutierrez M, Turner ML. Keratoacanthomas associated with sorafenib therapy. J Am Acad Dermatol. 2007; 56:171–2. [PubMed: 17190642]
8. Chapman PB, Hauschild A, Robert C, Haanen JB, Ascierto P, Larkin J, et al. Improved survival with vemurafenib in melanoma with BRAF V600E mutation. N Engl J Med. 2011; 364:2507–16. [PubMed: 21639808]
9. Flaherty KT, Puzanov I, Kim KB, Ribas A, McArthur GA, Sosman JA, et al. Inhibition of mutated, activated BRAF in metastatic melanoma. N Engl J Med. 2010; 363:809–19. [PubMed: 20818844]
10. Sosman JA, Kim KB, Schuchter L, Gonzalez R, Pavlick AC, Weber JS, et al. Survival in BRAF V600-mutant advanced melanoma treated with vemurafenib. N Engl J Med. 2012; 366:707–14. [PubMed: 22356324]
11. Heidorn SJ, Milagre C, Whittaker S, Nourry A, Niculescu-Duvas I, Dhomen N, et al. Kinase-dead BRAF and oncogenic RAS cooperate to drive tumor progression through CRAF. Cell. 2010; 140:209–21. [PubMed: 20141835]
12. Hatzivassiliou G, Song K, Yen I, Brandhuber BJ, Anderson DJ, Alvarado R, et al. RAF inhibitors prime wild-type RAF to activate the MAPK pathway and enhance growth. Nature. 2010; 464:431–5. [PubMed: 20130576]
13. Poulikakos PI, Zhang C, Bollag G, Shokat KM, Rosen N. RAF inhibitors transactivate RAF dimers and ERK signalling in cells with wild-type BRAF. Nature. 2010; 464:427–30. [PubMed: 20179705]
14. Karreth FA, DeNicola GM, Winter SP, Tuveson DA. C-Raf inhibits MAPK activation and transformation by B-Raf(V600E). Mol Cell. 2009; 36:477–86. [PubMed: 19917255]
15. Halaban R, Zhang W, Bacchiocchi A, Cheng E, Parisi F, Ariyan S, et al. PLX4032, a selective BRAF(V600E) kinase inhibitor, activates the ERK pathway and enhances cell migration and proliferation of BRAF melanoma cells. Pigment Cell Melanoma Res. 2010; 23:190–200. [PubMed: 20149136]
16. Su F, Viros A, Milagre C, Trunzer K, Bollag G, Spleiss O, et al. RAS mutations in cutaneous squamous-cell carcinomas in patients treated with BRAF inhibitors. N Engl J Med. 2012; 366:207–15. [PubMed: 22256804]
17. Oberholzer PA, Kee D, Dziunycz P, Sucker A, Kamsukom N, Jones R, et al. RAS Mutations Are Associated With the Development of Cutaneous Squamous Cell Tumors in Patients Treated With RAF Inhibitors. J Clin Oncol. 2011
18. Flaherty KT, Infante JR, Daud A, Gonzalez R, Kefford RF, Sosman J, et al. Combined BRAF and MEK Inhibition in Melanoma with BRAF V600 Mutations. N Engl J Med. 2012
19. Weber JS, Flaherty KT, Infante JR, Falchook GS, Kefford R, Daud A, et al. Updated safety and efficacy results from a phase I/II study of the oral BRAF inhibitor dabrafenib (GSK2118436) combined with the oral MEK 1/2 inhibitor trametinib (GSK1120212) in patients with BRAFi-naive metastatic melanoma. J Clin Oncol. 2012:30. [PubMed: 23169502]
20. Tournier C, Hess P, Yang DD, Xu J, Turner TK, Nimnual A, et al. Requirement of JNK for stress-induced activation of the cytochrome c-mediated death pathway. Science. 2000; 288:870–4. [PubMed: 10797012]

21. Haeusgen W, Herdegen T, Waetzig V. The bottleneck of JNK signaling: molecular and functional characteristics of MKK4 and MKK7. Eur J Cell Biol. 2011; 90:536–44. [PubMed: 21333379]
22. Tournier C, Whitmarsh AJ, Cavanagh J, Barrett T, Davis RJ. Mitogen-activated protein kinase kinase 7 is an activator of the c-Jun NH2-terminal kinase. Proc Natl Acad Sci U S A. 1997; 94:7337–42. [PubMed: 9207092]
23. Yang D, Tournier C, Wysk M, Lu HT, Xu J, Davis RJ, et al. Targeted disruption of the MKK4 gene causes embryonic death, inhibition of c-Jun NH2-terminal kinase activation, and defects in AP-1 transcriptional activity. Proc Natl Acad Sci U S A. 1997; 94:3004–9. [PubMed: 9096336]
24. Haass NK, Sproesser K, Nguyen TK, Contractor R, Medina CA, Nathanson KL, et al. The mitogen-activated protein/extracellular signal-regulated kinase kinase inhibitor AZD6244 (ARRY-142886) induces growth arrest in melanoma cells and tumor regression when combined with docetaxel. Clin Cancer Res. 2008; 14:230–9. [PubMed: 18172275]
25. Inaba H, Rubnitz JE, Coustan-Smith E, Li L, Furmanski BD, Mascara GP, et al. Phase I pharmacokinetic and pharmacodynamic study of the multikinase inhibitor sorafenib in combination with clofarabine and cytarabine in pediatric relapsed/refractory leukemia. J Clin Oncol. 2011; 29:3293–300. [PubMed: 21768474]
26. Davis MI, Hunt JP, Herrgard S, Ciceri P, Wodicka LM, Pallares G, et al. Comprehensive analysis of kinase inhibitor selectivity. Nat Biotechnol. 2011; 29:1046–51. [PubMed: 22037378]
27. Keshet Y, Seger R. The MAP kinase signaling cascades: a system of hundreds of components regulates a diverse array of physiological functions. Methods Mol Biol. 2010; 661:3–38. [PubMed: 20811974]
28. Yang JJ. Mixed lineage kinase ZAK utilizing MKK7 and not MKK4 to activate the c-Jun N-terminal kinase and playing a role in the cell arrest. Biochem Biophys Res Commun. 2002; 297:105–10. [PubMed: 12220515]
29. Sauter KA, Magun EA, Iordanov MS, Magun BE. ZAK is required for doxorubicin, a novel ribotoxic stressor, to induce SAPK activation and apoptosis in HaCaT cells. Cancer Biol Ther. 2010; 10:258–66. [PubMed: 20559024]
30. Wong J, Smith LB, Magun EA, Engstrom T, Kelley-Howard K, Jandhyala DM, et al. Small molecule kinase inhibitors block the ZAK-dependent inflammatory effects of doxorubicin. Cancer Biol Ther. 2013; 14:56–63. [PubMed: 23114643]
31. de Anda FC, Rosario AL, Durak O, Tran T, Graff J, Meletis K, et al. Autism spectrum disorder susceptibility gene TAOK2 affects basal dendrite formation in the neocortex. Nat Neurosci. 2012; 15:1022–31. [PubMed: 22683681]
32. Wu MF, Wang SG. Human TAO kinase 1 induces apoptosis in SH-SY5Y cells. Cell Biol Int. 2008; 32:151–6. [PubMed: 17900936]
33. Chen Z, Cobb MH. Regulation of stress-responsive mitogen-activated protein (MAP) kinase pathways by TAO2. J Biol Chem. 2001; 276:16070–5. [PubMed: 11279118]
34. Zihni C, Mitsopoulos C, Tavares IA, Ridley AJ, Morris JD. Prostate-derived sterile 20-like kinase 2 (PSK2) regulates apoptotic morphology via C-Jun N-terminal kinase and Rho kinase-1. J Biol Chem. 2006; 281:7317–23. [PubMed: 16407310]
35. Moore TM, Garg R, Johnson C, Coptcoat MJ, Ridley AJ, Morris JD. PSK, a novel STE20-like kinase derived from prostatic carcinoma that activates the c-Jun N-terminal kinase mitogen-activated protein kinase pathway and regulates actin cytoskeletal organization. J Biol Chem. 2000; 275:4311–22. [PubMed: 10660600]
36. Heinrich MC, Marino-Enriquez A, Presnell A, Donsky RS, Griffith DJ, McKinley A, et al. Sorafenib inhibits many kinase mutations associated with drug-resistant gastrointestinal stromal tumors. Mol Cancer Ther. 2012; 11:1770–80. [PubMed: 22665524]

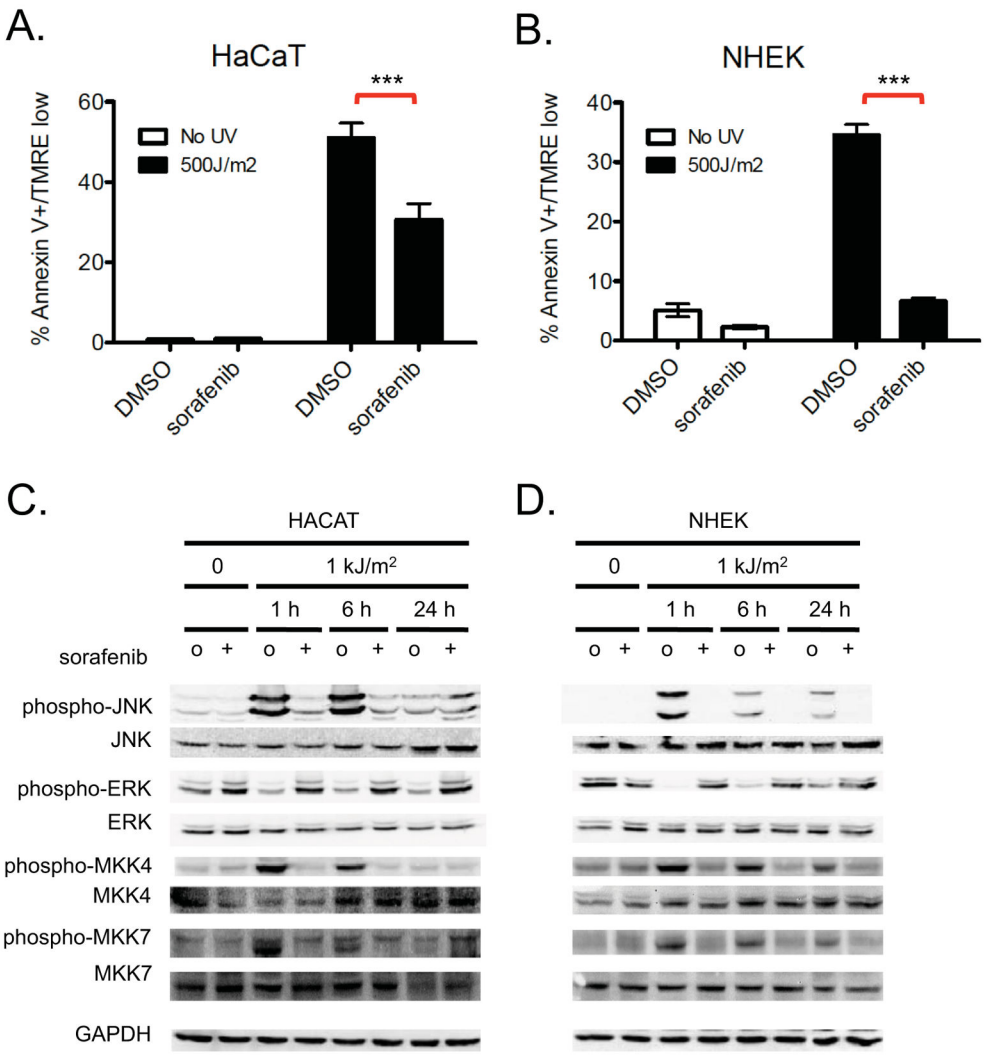

Figure 1. Sorafenib suppresses UV-induced apoptosis

HaCaT and NHEK cells were either unirradiated or irradiated with 500 J/m^2 of UVB in the absence ("o", 1:2000 DMSO) or presence ("+") of 1 μM sorafenib and isolated for FACS analysis and protein extracts 24 hours later. **A**, HaCaT, **B**, NHEK cells show 45% and 80% suppression, respectively, of apoptosis in the presence of sorafenib as measured by FACS for Annexin V+, TMRE-low cells (n=6 for each condition, "***", $p<0.001$). Western blots of HaCaT (**C**) and NHEK (**D**) cells probed for the MAP kinases JNK and ERK demonstrated strong phospho-JNK induction following irradiation and significant suppression by sorafenib. Phospho-ERK was slightly suppressed following irradiation, and at all time points, paradoxical hyperactivation in the presence of sorafenib was observed, particularly in HaCaT cells. Importantly, phospho-MKK4 and phospho-MKK7, upstream kinases that activate JNK, were both strongly induced by UV radiation and strongly suppressed by sorafenib.

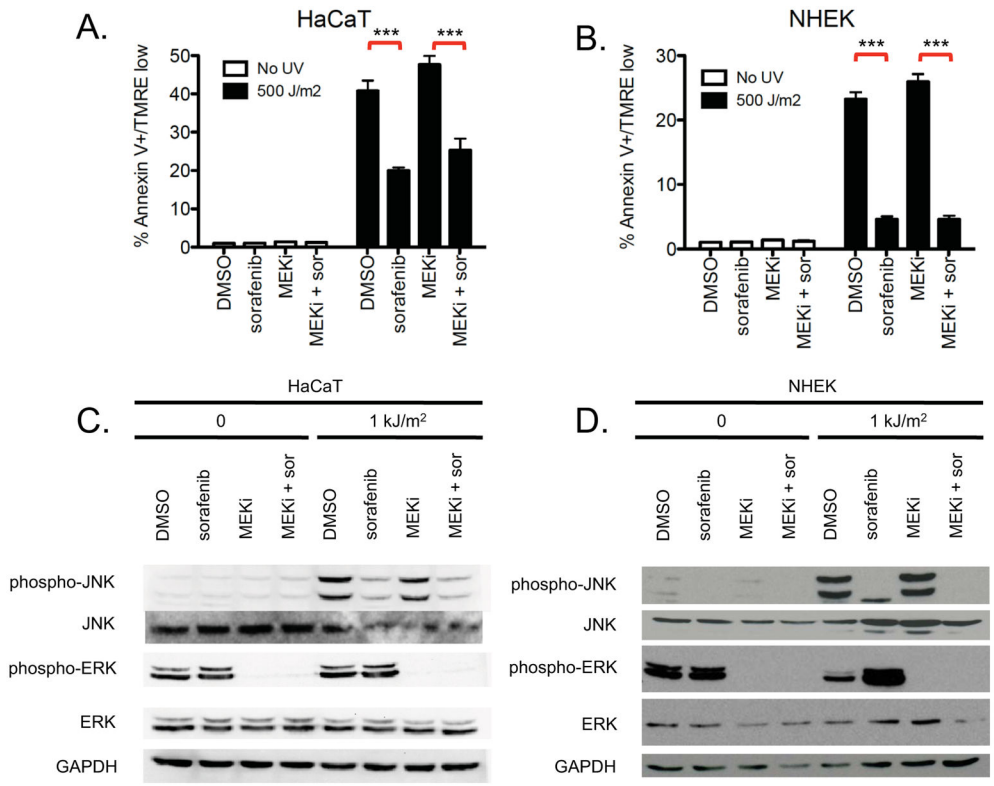

Figure 2. Sorafenib suppresses apoptosis and JNK signaling independently of MEK/ERK signaling

To test the relevance of MEK/ERK signaling in the suppression of JNK-mediated apoptosis, HaCaT and NHEK cells were irradiated with 500 J/m^2 of UVB in the absence ("o", 1:2000 DMSO) or presence of 1 μM sorafenib singly or in combination with 0.6 μM (NHEK) or 1.2 μM (HaCaT) selumetinib (MEKi) and isolated for FACS analysis and protein extracts 24 hours later. **A**, HaCaT and **B**, NHEK cells exhibited a strong suppression of UV-induced apoptosis by sorafenib (Annexin V+, TMRE-low cells; n=6 for each condition, "***", $p<0.001$) that was not substantially by the addition of MEKi. **C**, HaCaT and **D**, NHEK cells showed induction of phospho-JNK at 24 hours following irradiation, by Western in the presence (lane 7) and absence (lane 5) of MEKi. The addition of MEKi with sorafenib did not affect the suppression of JNK activation (compare lanes 7 vs. 8) despite potent suppression of phospho-ERK.

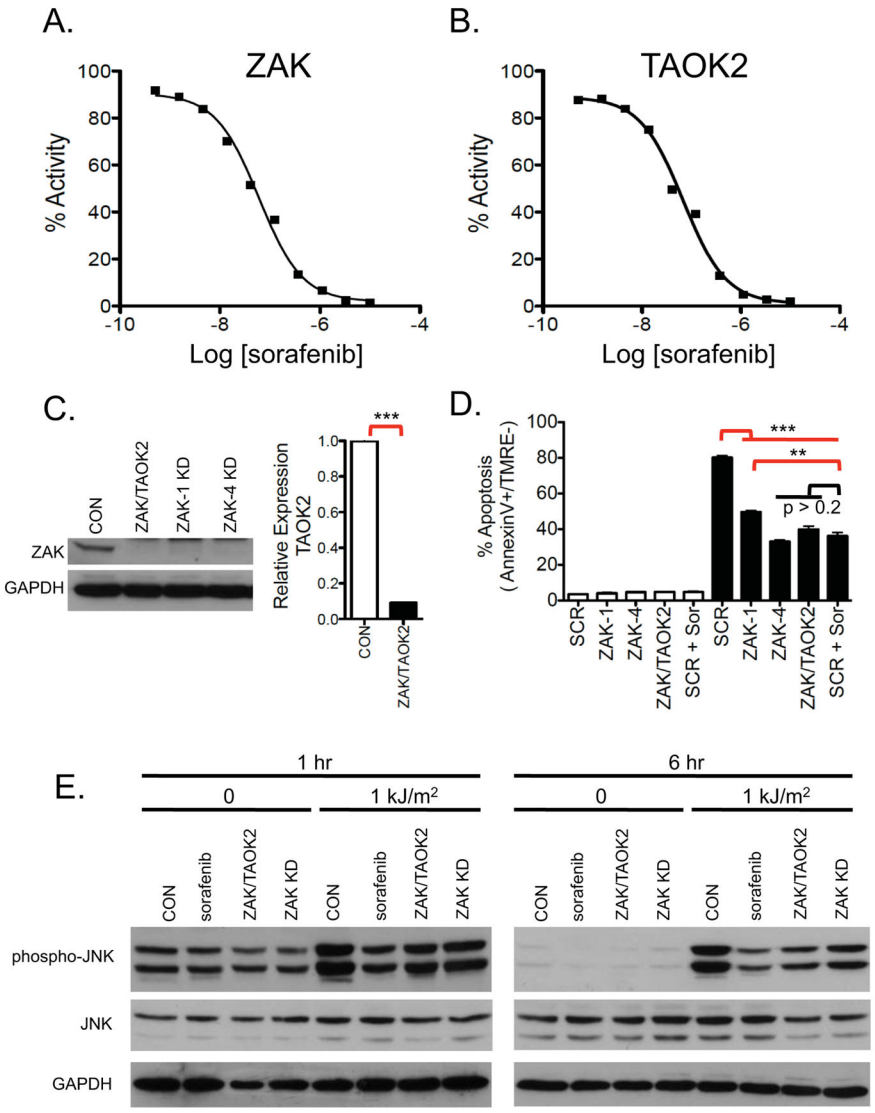

Figure 3. Sorafenib exhibits significant off-target effects on ZAK and TAOK2 kinases

A–B, *In-vitro* kinase assays for ZAK and TAOK2 were performed across a 10-point concentration range from 0.03 to 10μM, revealed significant inhibition of kinase activity within the nM range for sorafenib. **C.** Lentiviral shRNA knockdown of ZAK singly (clones ZAK-1, ZAK-4) or in combination with TAOK2 was performed, with both exhibiting significant knockdown of ZAK protein. Knockdown of TAOK2 was quantitated using Taqman qRT-PCR, showing 91% knockdown ("***", $p<0.001$) **D,** Lentiviral shRNA knockdown of ZAK singly (two clones ZAK-1 and ZAK-4) or in combination with TAOK2 (ZAK-1 only) was performed, revealing potent suppression of apoptosis as measured by FACS for Annexin V+, TMRE-low cells (n=9, "*", $p<0.05$, "**"; $p<0.01$; "NS" is not significant) at 24 hours following single dose UVB irradiation at 1 kJ/m^2. ZAK single knockdowns exhibited 38% (ZAK-1) and 59% (ZAK-4) suppression whereas ZAK/TAOK2 double knockdown cells and drug-treated cells exhibited 50% and 55% suppression of apoptosis, respectively. Differences between the ZAK-4 shRNA single knockdown, ZAK/

TAOK2 double knockdown, and sorafenib-treated scramble (“SCR”) cells were not statistically significant. **E**, Western blots of lysates obtained at 1 and 6 hours post-UV irradiation show potent induction of phospho-JNK following UV irradiation (both lanes 5). ZAK-1 shRNA single knockdown produced suppression of phospho-JNK activation comparable to those of ZAK/TAOK2 double knockdown and sorafenib treatment (lanes 6–8).

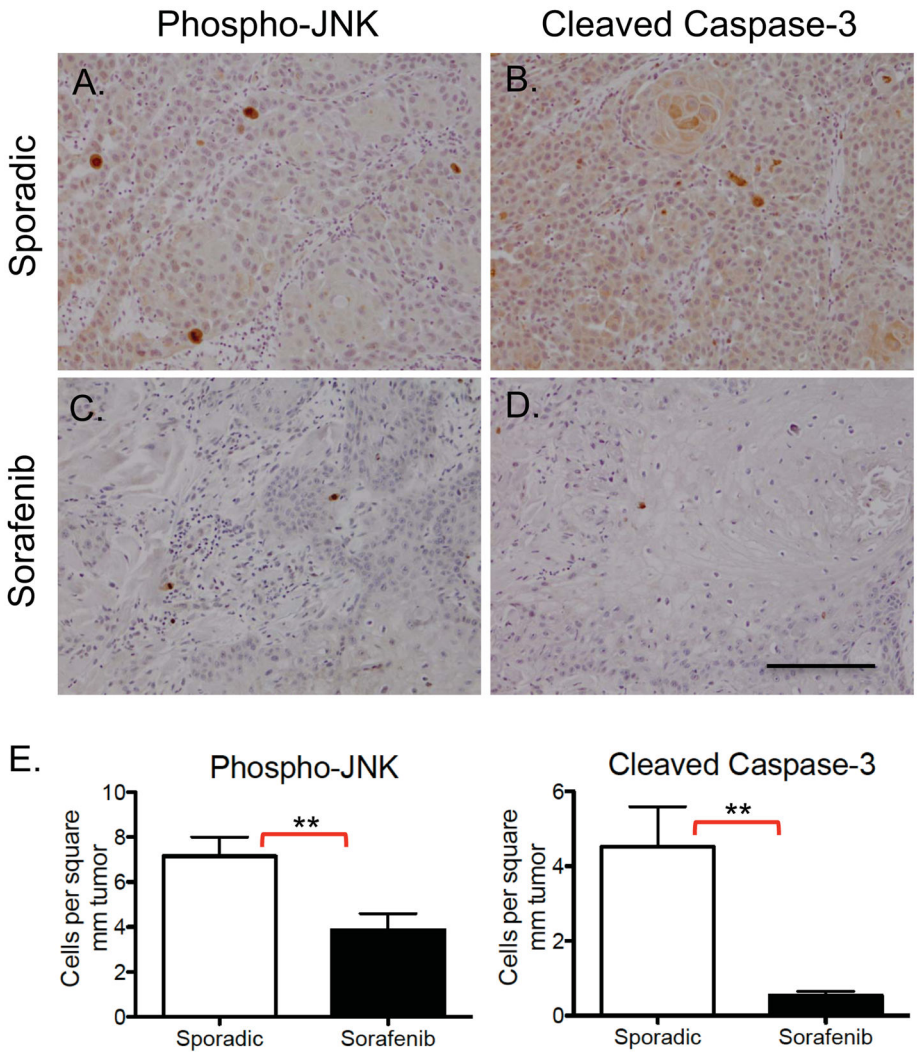

Figure 4. Sorafenib suppresses apoptosis and JNK signaling *in-vivo*

A–D, cSCC samples from sorafenib-treated patients and non-treated patients ("sporadic") were analyzed by immunohistochemistry for phospho-JNK and cleaved caspase-3 expression. cSCC arising in sorafenib-treated patients show decreased expression of phospho-JNK (**C**) and cleaved caspase-3 (**D**) as compared to sporadic cSCC in patients never treated with sorafenib (**A, B**). Scale bar is 100 μm. **E,** Comparisons of stained cells normalized to mm^2 of tumor area revealed significant suppression of both phospho-JNK and cleaved caspase 3 expression in sorafenib-treated cSCC ("**", $p<0.01$).

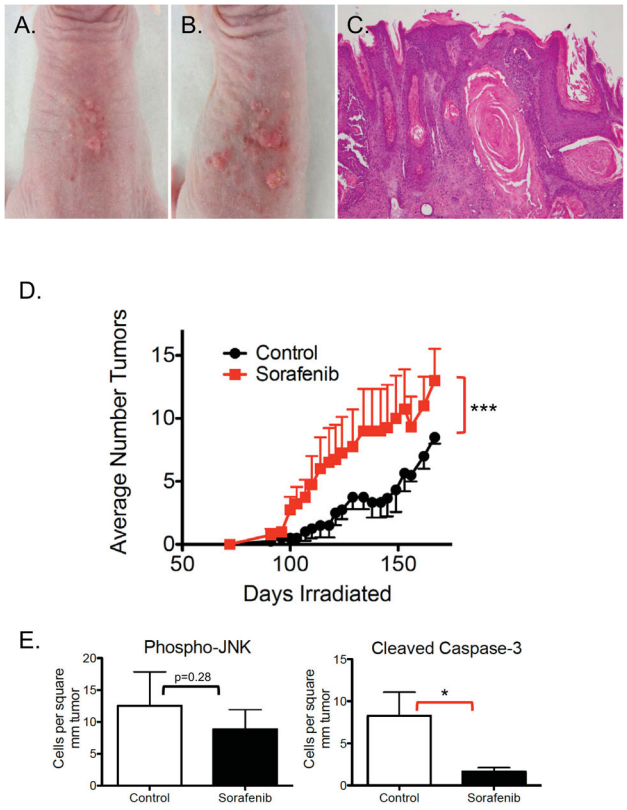

Figure 5. Sorafenib increases cSCC development in the UV-driven Hairless mouse model

A–E, Chronically-irradiated Hairless mice were treated with sorafenib (n=5) and vehicle (n=5) starting at day 72 (**D**). Tumors were induced within 30 days of sorafenib treatment (**A, B, D**). Although tumors exhibited similar kinetics, there were 2.3-fold more tumors in sorafenib-treated mice (**B**, day 120) as compared to vehicle-treated mice (**A**, day 120) on average (**D,** "***", $p<0.001$). **E**, Tumors from sorafenib-treated animals showed lower levels of phospho-JNK ($p=0.28$) and cleaved caspase 3 ($p=0.03$, "*" $p < 0.05$) as compared to control-treated animals (n=6 pairs).

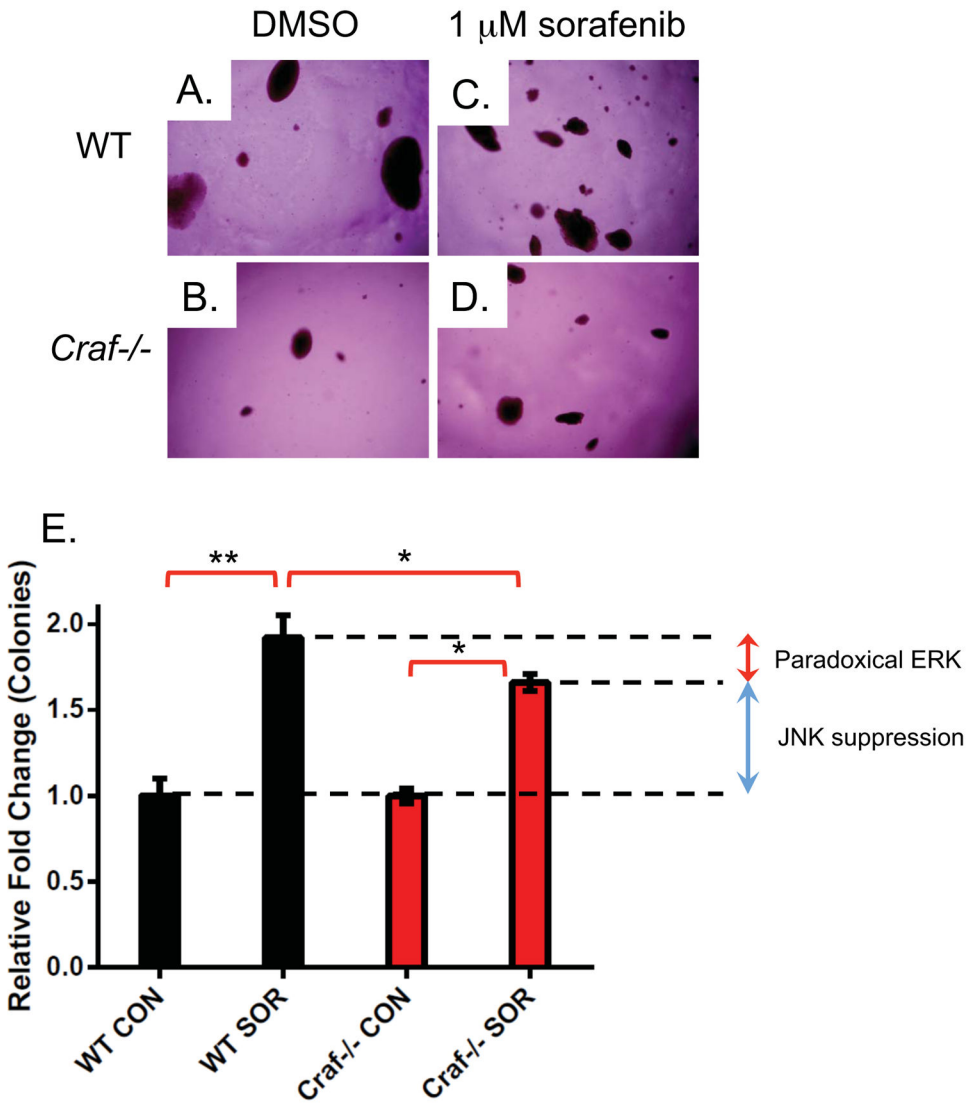

Figure 6. Paradoxical ERK activation and JNK pathway inhibition make significant and separable contributions to sorafenib-induced growth

A–E, We envision two separable, parallel mechanisms by which sorafenib contributes to cSCC development. Drug-induced paradoxical ERK activation and inhibition of JNK signaling occur in parallel, but the former depends on intact *CRAF*. **A–D,** Representative soft agar colonies of E1A and *HRAS*^{G12V}-transformed wild-type (WT) (**A**) and *Craf*−/− (**B**) MEFs, following exposure to 1.0 μM sorafenib (**C, D**) over 4–6 weeks show significant colony-forming advantages conferred by sorafenib. **E**, The fold-change in colony counts of transformed wild-type (WT) (n=36) and *Craf*−/− (n=22) MEFs demonstrate a drug-induced increase in colonies, for both WT (1.92-fold) and *Craf*−/− (1.66-fold) MEFs. The difference between colony formation advantages conferred by 1.0 μM sorafenib in WT vs. *Craf*−/− MEFs was interpreted to reflect the contribution of paradoxical ERK signaling (red arrow), which depends upon *Craf*, and is 13.5% of the total effect reflected in the first two columns. The remainder of the total effect is composed of other effects including JNK inhibition (blue

arrow). All differences within each MEF population were significant (“*”, $p<0.05$; “**”, $p<0.01$).